Published OnlineFirst October 16, 2020; DOI: 10.1158/0008-5472.CAN-20-1161

Hes1 Is Essential in Proliferating Ductal Cell–Mediated Development of Intrahepatic Cholangiocarcinoma

Tomoaki Matsumori[1], Yuzo Kodama[1,2], Atsushi Takai[1], Masahiro Shiokawa[1], Yoshihiro Nishikawa[1], Tomonori Matsumoto[3], Haruhiko Takeda[1], Saiko Marui[1], Hirokazu Okada[1], Tomonori Hirano[1], Takeshi Kuwada[1], Yuko Sogabe[1], Nobuyuki Kakiuchi[1], Teruko Tomono[1], Atsushi Mima[1], Toshihiro Morita[1], Tatsuki Ueda[1], Motoyuki Tsuda[1], Yuki Yamauchi[1], Katsutoshi Kuriyama[1], Yojiro Sakuma[1], Yuji Ota[1], Takahisa Maruno[1], Norimitsu Uza[1], Hiroyuki Marusawa[4], Ryoichiro Kageyama[5], Tsutomu Chiba[1,6], and Hiroshi Seno[1]

ABSTRACT

Intrahepatic cholangiocarcinoma (ICC) is frequently driven by aberrant *KRAS* activation and develops in the liver with chronic inflammation. Although the Notch signaling pathway is critically involved in ICC development, detailed mechanisms of Notch-driven ICC development are still unknown. Here, we use mice whose Notch signaling is genetically engineered to show that the Notch signaling pathway, specifically the Notch/Hes1 axis, plays an essential role in expanding ductular cells in the liver with chronic inflammation or oncogenic *Kras* activation. Activation of Notch1 enhanced the development of proliferating ductal cells (PDC) in injured livers, while depletion of *Hes1* led to suppression. In correlation with PDC expansion, ICC development was also regulated by the Notch/Hes1 axis and suppressed by *Hes1* depletion. Lineage-tracing experiments using *Epcam*^{creERT2} mice further confirmed that Hes1 plays a critical role in the induction of PDC and that ICC could originate from PDC. Analysis of human ICC specimens showed PDC in nonneoplastic background tissues, confirming HES1 expression in both PDC and ICC tumor cells. Our findings provide novel direct experimental evidence that Hes1 plays an essential role in the development of ICC via PDC.

Significance: This study contributes to the identification of the cells of origin that initiate ICC and suggests that HES1 may represent a therapeutic target in ICC.

Introduction

Intrahepatic cholangiocarcinoma (ICC) is one of the most frequent primary cancers in the liver and has a high worldwide mortality (1). Chronic viral hepatitis and steatohepatitis, generally due to lifestyle and habits, are known to be one of the causes of the development of ICC and hepatocellular carcinoma (HCC; ref. 2). Chronic infection with liver flukes is also a risk factor for ICC (3, 4). Cancers in the inflamed liver originate from proliferating liver cells with accumulation of genetic alterations, which are mediated by inflammation (5). Recent genome analyses of human ICCs revealed that genetic aberrations in *KRAS, TP53*, and *IDH1/2* are the most critical drivers of ICC (6, 7). Consistently, genetically modified mice, whose hepatocytes harbor oncogenic mutations in *Kras* and *Trp53* genes, developed ICCs (8, 9). *Trp53* deficiency with oncogenic *Kras* mutation also induced ICCs derived from both cholangiocytes and hepatocytes (10). These findings suggest that ICC originates from proliferating liver cells with *KRAS* and *TP53* mutations localized in chronically injured livers.

Notch signaling is also closely involved in ICC development. Notch signaling regulates cell growth and differentiation in the embryonic and adult livers and plays important roles in liver development, homeostasis, and diseases (11, 12). Among Notch signaling–related molecules, recent reports have shown the important roles of Notch2 receptor in ICC development (13–15), and their main effectors including Hairy and enhancer of split1 (HES1) are upregulated in human ICCs (16). In addition, liver-specific overexpression of Notch1 promoted ICC development in mice (16–19), whereas inhibition of HES1 suppressed the growth of various tumors, including human pancreatic ductal adenocarcinoma (20, 21). These findings suggest that Notch signaling, particularly the Notch/Hes1 axis, contributes to the development of ICC, although it remains unclear whether Hes1 expression directly affects ICC development.

Whether HCC and ICC are derived from differentiated hepatocytes, cholangiocytes, or other cells is still controversial (22–24). Proliferating ductal cells (PDC), which are often observed in chronically inflamed livers as ductular reactions and are facultative liver stem/progenitor cells (25–27), constitute another potential source of liver cancers (22, 24, 28). Our previous study, which labeled and traced PDCs in genetically engineered mouse models, demonstrated that PDCs gave rise to HCCs with upregulation of the Wnt signaling pathway in chronically inflamed livers without abnormal expression of the Notch signaling pathway in PDCs (28). Moreover, PDCs in the inflamed liver also exhibit enhanced expression of Notch signaling effectors (29). Given that PDCs have malignant potential and their proliferation is significantly increased with Notch signaling activation, they could be an important origin of ICC.

[1]Department of Gastroenterology and Hepatology, Kyoto University Graduate School of Medicine, Kyoto, Japan. [2]Department of Gastroenterology, Kobe University Graduate School of Medicine, Hyogo, Japan. [3]Oregon Stem Cell Center, Oregon Health and Science University, Portland, Oregon. [4]Department of Gastroenterology, Japanese Red Cross Hospital Osaka, Osaka, Japan. [5]Institute for Frontier Life and Medical Sciences, Kyoto University, Shogoin-Kawahara, Sakyo-Ku, Kyoto, Japan. [6]Kansai Electric Power Hospital, Osaka, Japan.

Note: Supplementary data for this article are available at Cancer Research Online (http://cancerres.aacrjournals.org/).

Corresponding Author: Yuzo Kodama, Kobe University Graduate School of Medicine, 7-5-1 Kusunoki-cho, Chuo-ku, Kobe, Hyogo 650-0017, Japan. Phone: 81783826305; Fax: 81783826309; E-mail: kodama@med.kobe-u.ac.jp

Cancer Res 2020;80:5305–16

doi: 10.1158/0008-5472.CAN-20-1161

Published OnlineFirst October 16, 2020; DOI: 10.1158/0008-5472.CAN-20-1161

In the present study, we investigated the role of *Hes1* in the development of ICC using genetically engineered mouse models in which *Hes1* was explicitly deleted or upregulated in the liver or PDCs. We found that the Notch/Hes1 axis critically regulates the development of both PDCs and ICCs. Furthermore, lineage tracing analysis confirmed that ICC develops from PDCs overexpressing Hes1. Our findings indicate that Hes1 plays an essential role in the development of ICC via PDCs and suggest the Notch/Hes1 axis as a promising new target for ICC treatment.

Materials and Methods

Human samples

Immunohistological analyses were performed on surgically resected specimens from 25, 21, and 5 admitted patients with ICC, HCC, and metastatic liver cancers, respectively, at Kyoto University Hospital (Kyoto, Japan). The Ethics Committee of Kyoto University approved the current study's protocol. We have complied with all relevant ethical regulations. Informed consent was obtained from all participants.

Animals

Alb-Cre Tg mice (30), *Hes1 flox* mice (31), *LSL-Kras*^{G12D} mice (32), *LSL-Trp53*^{R172H} mice (33), *Rosa26-CAG-LSL-tdTomato-WPRE* mice (34), *Epcam-CreER*^{T2} *Tg* mice (28), and mice overexpressing the *Notch1*-intracellular domain (35) have been described. We obtained *Alb-Cre Tg* mice, *LSL-Kras*^{G12D} mice, and *Rosa26-CAG-LSL-tdTomato-WPRE* mice from The Jackson Laboratory. *LSL-Trp53*^{R172H} mice were kindly gifted from Dr. Tyler Jacks (Center for Cancer Research, Massachusetts Institute of Technology, Cambridge, MA). *Notch1*-intracellular domain–overexpressed mice were kindly gifted from Dr. Douglas A Melton (Department of Stem cell and Regenerative Biology, Harvard University, Cambridge, MA). *Epcam-CreER*^{T2} *Tg* mice (Department of Gastroenterology and Hepatology, Kyoto University Graduate School of Medicine, Kyoto, Japan) and *Hes1 flox* mice (Institute for Frontier Life and Medical Sciences, Kyoto University, Kyoto, Japan) were generated in our institute. Mice were maintained in a specific pathogen-free facility at the Kyoto University Faculty of Medicine (Kyoto, Japan). Mice were of mixed genetic backgrounds, and there was no specific sex selection in this study. All mouse strains (*Alb*^{cre}, *Epcam*^{creERT2}, *Kras*^{G12D}, *Trp53*^{R172H}, *Hes1*$^{flox/flox}$, *Rosa*^{tdTomato}, *Rosa*^{NotchOE}) have been studied previously. In all mice experiments, the mice were monitored for signs of illness including abdominal bloating, diminished activity, and/or poor grooming. All animal experiments were approved by the Ethics Committee for Animal Experiments and performed under the Guidelines for Animal Experiments of Kyoto University.

Production of PDCs was induced by feeding 4-week-old mice with chow containing 0.1% (w/w) 3,5-diethoxycarbonyl-1,4-dihydrocollidine (DDC, Sigma-Aldrich) for 1 to 5 months. Tamoxifen (Sigma-Aldrich) was dissolved in corn oil (Wako) at a concentration of 20 mg/mL and i.p. injected into 6- to 8-week-old mice at a dose of 150 mg/kg body weight.

Histologic analyses

Liver tissues were fixed with 10% neutral phosphate-buffered formalin and embedded in paraffin or optimum cutting temperature compound (Leica Instruments). Paraffin-embedded tissues were sectioned and stained with hematoxylin and eosin or following primary antibodies for both mouse and human specimens: rabbit anti-cytokeratin 19 (1:200 dilution; ab52625, Abcam), rabbit anti-Sox9 (1:20,000 dilution; AB5535, Merck Millipore), and rabbit anti-Hes1 (gift from Dr. Tetsuo Sudo, Toray Industries; ref. 36). Sections were incubated with primary antibodies overnight at 4°C and stained using an EnVision+ kit (Dako) or LSAB2 kit (Dako), and VECTASTAIN Elite ABC kit (Vector Laboratories) according to the manufacturer's instructions. The peroxidase reaction was performed with Liquid DAB+ Substrate Chromogen System (Dako). Slides were counterstained with hematoxylin (Wako). Primary antibodies used for immunofluorescence of mouse specimens were: rabbit anti-cytokeratin 19 (Keratin 19; 1:200 dilution; ab52625, Abcam), goat anti-cytokeratin19 (Keratin19; 1:100 dilution; sc-33111, Santa Cruz Biotechnology), rat anti-Epcam (1:200 dilution; ab92382, Abcam), goat anti-Hnf4α (1:250 dilution; sc-6556, Santa Cruz Biotechnology), rat anti-Ki67 (1:100 dilution; 16A8, BioLegend), rabbit anti–phospho-p44/42 MAPK (Erk1/2) (Thr202/Try204) (D13.14.4E) XP (1:400 dilution; #4370, Cell Signaling Technology), and goat anti-Trop2 (1:40 dilution; AF1122, R&D Systems). Frozen sections were stained with primary antibodies and fluorescence-conjugated secondary antibodies (Thermo Fisher Scientific; Jackson Laboratories; or Sigma-Aldrich). Nuclei were visualized by Hoechst staining (Thermo Fisher Scientific).

Morphometric quantification

The ratio of each Krt19-, Epcam-, Trop2-, and tdTomato-positive area to the total area within sections was analyzed using ImageJ software (National Institutes of Health, Bethesda, MD; https://imagej.nih.gov/ij/).

Quantitative RT-PCR

Total RNA was extracted from liver tissues collected in RNAlater (Ambion) using an RNeasy kit (QIAGEN) according to the manufacturer's instruction. For complementary DNA synthesis, 1 μg of total RNA was reverse-transcribed using ReverTra Ace qPCR RT Master Mix (Toyobo) and subjected to quantitative RT-PCR (qRT-PCR) using the LightCycler system (Roche), FastStart Universal SYBR Green Master (Roche), and the primers listed in Supplementary Table S1. Expression levels of specific genes were normalized to that of the housekeeping gene, glyceraldehyde 3-phosphate dehydrogenase. All qRT-PCR samples were evaluated in technical triplicate.

RNA sequencing

RNA sequencing (RNA-seq) was conducted with Novaseq 6000 platform (Illumina). RNA-seq generated 100-bp paired-end sequences, and these raw reads were aligned to the reference genome sequence (http://genome.ucsc.edu/, GRCm38/mm10) using HISAT2. Total mapped raw read numbers of each gene were calculated using Stringtie, and differential expression analysis of each group was conducted with trimmed mean of M values (TMM) normalization and edgeR program in the default setting using R v.4.0.1. Genes with both a P value of less than 0.05 and an FDR of less than 0.1 were considered to be significantly differentially expressed genes (DEG). Gene set enrichment analysis (GSEA) was performed using public software obtained from Broad Institute to compare the gene expression profile of each case. Heatmap was constructed by using Z-scored log2(normalized mapped read). Sequence data were deposited at the DNA data Bank of Japan Sequence Read Archive (DRA), under accession number DRA010539.

Statistical analysis

Statistical analysis employed JMP (SAS Institute), GraphPad Prism7 (GraphPad Software,), and Excel (Microsoft Corp) software. We used the two-tailed Student t test and χ^2 tests to analyze differences between two groups for continuous and categorical data, respectively. Any values of $P < 0.05$ were considered as statistically significant and denoted as *, $P < 0.05$ or **, $P < 0.01$. Data were presented as the mean ± SEM (or mean ± SD).

Published OnlineFirst October 16, 2020; DOI: 10.1158/0008-5472.CAN-20-1161

Results

Hes1-positive PDCs are increased prior to development of *Kras*-driven ICC

To analyze Hes1 expression during ICC development, we established two *Kras*-driven ICC mouse models by crossing Alb^{cre} mice with *LSL-Kras*^{G12D} (*K*) and *LSL-Trp53*^{R172H} (*P*) mice to generate $Alb^{cre}K$ and $Alb^{cre}KP$ mice (**Fig. 1A**). Cre recombinase driven by *Alb* gene promoter is expressed in embryonic hepatoblasts in these mice, and genetically modified hepatoblasts are supposed to give rise to all liver epithelial cell lineages, including hepatocytes, cholangiocytes, and PDCs in adult mice. In control Alb^{cre} mice, Krt19-positive biliary epithelial cells expressing Hes1 protein were observed in the normal intrahepatic bile ducts in the portal areas (Supplementary Fig. S1A). Trop2, a known PDC-specific marker (37, 38), was not expressed in these biliary epithelial cells (Supplementary Fig. S1A). In contrast, the expansion of ductal cells positive for Krt19, Hes1, and Trop2 was observed in the liver of 32-week-old $Alb^{cre}K$; $Hes1^{WT/WT}$ mice, without any tumor formation (**Fig. 1B**, top plots). Furthermore, more than 60% of $Alb^{cre}K$; $Hes1^{WT/WT}$ mice developed both ICCs (63.6%, 7/11) and HCCs (63.6%, 7/11) at 48 weeks of age, and those ICCs were also positive for Krt19, Trop2, and Hes1 (**Fig. 1B**, bottom plots). As with the $Alb^{cre}K$ mice, $Alb^{cre}KP$ mice developed PDCs and ICCs (25.0%, 5/20) as early as at 16 and 20 weeks of age in $Alb^{cre}KP$ mice, respectively. PDCs (**Fig. 1C**, top plots) and ICCs (**Fig. 1C**, bottom plots) in $Alb^{cre}KP$ mice were also positive for Krt19, Trop2, and Hes1. In control Alb^{cre} mice, neither PDCs nor liver tumors were observed in the background liver at 48 weeks of age (Supplementary Fig. S1B). Thus, in our *Kras*-driven mouse models, PDC expansion was observed prior to ICC development, and both ICC and PDCs expressed Hes1 and other PDC markers.

Hes1 plays an important role in inducing PDC formation and ICC development

To assess the role of Hes1 in healthy liver development, we first generated liver-specific *Hes1* knockout mice by crossing Alb^{cre} mice and $Hes1^{flox/flox}$ mice (Supplementary Fig. S1C). The *Hes1* gene was efficiently deleted in the liver of Alb^{cre}; $Hes1^{flox/flox}$ mice, but this did not affect mouse body weight, liver weight, and bile duct formation, indicating that *Hes1* knockout did not affect the normal liver and bile duct development (Supplementary Fig. S1D–S1F).

Next, to evaluate the role of Hes1 in *Kras*-driven PDC induction and ICC development, we crossed $Alb^{cre}K$ or $Alb^{cre}KP$ mice with $Hes1^{flox/flox}$ mice for liver-specific *Hes1* depletion (**Fig. 2A**). Assessment of the Krt19- or Trop2-positive area by IHC revealed significant attenuation of PDC formation in $Alb^{cre}KP$; $Hes1^{flox/flox}$ mice compared with that in $Alb^{cre}KP$; $Hes1^{WT/WT}$ mice (**Fig. 2B**). Consistently, *Krt19* and *Trop2* mRNA levels in the liver were also significantly decreased in $Alb^{cre}KP$; $Hes1^{flox/flox}$ mice compared with those in $Alb^{cre}KP$; $Hes1^{WT/WT}$ mice (**Fig. 2C**). Notably, *Hes1* deletion dramatically reduced ICC development in both $Alb^{cre}K$ mice (63.6% in $Hes1^{WT/WT}$ vs. 11.1% in $Hes1^{flox/flox}$ at 48 weeks of age, $P = 0.028$) and $Alb^{cre}KP$ mice (25% in $Hes1^{WT/WT}$ vs. 0% in $Hes1^{flox/flox}$ at 20 weeks of age, $P = 0.047$; **Fig. 2D**). In marked contrast, the frequency of HCC development was similar between $Alb^{cre}K$; $Hes1^{flox/flox}$ and $Alb^{cre}K$; $Hes^{WT/WT}$ mice (66.7% 6/9 vs. 63.6%, 7/11, $P = 0.742$) and between $Alb^{cre}KP$; $Hes1^{flox/flox}$ and $Alb^{cre}KP$; $Hes1^{WT/WT}$ mice (55.0%, 11/20 vs. 80.0%, 16/20, $P = 0.177$), indicating that *Hes1* knockout did not attenuate HCC development (Supplementary Fig. S2A). IHC staining showed that ICC and HCC formed in $Alb^{cre}K$; $Hes1^{flox/flox}$ and $Alb^{cre}KP$; $Hes1^{flox/flox}$ mice did not express Hes1 (Supplementary Fig. S2B). Taken together, in our *Kras*-driven mouse models, *Hes1* knockout significantly reduced both PDC formation and ICC development but did not affect HCC development, suggesting a close association between PDC formation and ICC development.

To explore the targets of Hes1 in PDC induction and ICC development, we performed RNA-seq using nonneoplastic background liver tissues of $Alb^{cre}K$; $Hes1^{WT/WT}$ and $Alb^{cre}K$; $Hes1^{flox/flox}$ mice. As a result, we identified 170 DEGs by RNA-seq (Supplementary Fig. S2C and S2D; Supplementary Table S2), and GSEA that the liver tissue of $Alb^{cre}K$; $Hes1^{flox/flox}$ mice had reduced expression of gene sets related with *Kras* activation (HALLMARK_KRAS_SIGNALING_UP), cell cycle (e.g., HALLMARK_E2F_TARGETS), and inflammation (e.g., TNFA_SIGNALING_VIA_NFKB) as compared with $Alb^{cre}K$ mice (**Fig. 2E**; Supplementary Fig. S2E; Supplementary Table S3). Despite the same status of mutant *Kras* between the two strains of mice, IHC showed reduced phosphorylation of Erk (pErk) and Ki67-positive cells in the liver epithelial cells of $Alb^{cre}K$; $Hes1^{flox/flox}$ mice, confirming the attenuation of RAS/ERK signaling and cell cycle compared with $Alb^{cre}K$ mice (Supplementary Fig. S2F). These data suggest that Hes1 plays a role in maintaining activation of the RAS/ERK pathway, which is required for proliferation of ductal cells and subsequent ICC formation.

Hes1 plays a central role in Notch-induced PDC formation and ICC development

To further examine the involvement of the Notch/Hes1 axis in ICC development, we genetically modified both Alb^{cre} and $Alb^{cre}KP$ mice to overexpress Hes1. First, Alb^{cre} mice were crossed with mice overexpressing the Notch1 intracellular domain (Alb^{cre}; $Rosa^{NotchOE/+}$ mice). Liver *Hes1* mRNA levels in these mice were higher than those of other transcriptional factors downstream of the Notch1 receptor (Supplementary Fig. S3), confirming that Hes1 is the main target of Notch1 in the liver. Next, we analyzed the involvement of Notch1 in PDC expansion and ICC development by crossing $Alb^{cre}KP$ mice and $Rosa^{NotchOE/+}$ mice (**Fig. 3A**). Nontumorous liver tissues of 8-week-old $Alb^{cre}KP$; $Rosa^{NotchOE/+}$ mice contained significantly higher numbers of PDCs expressing Hes1, Krt19, Trop2, and other duct/progenitor markers, such as Epcam and Sox9, than the tissues of $Alb^{cre}KP$ mice (**Fig. 3B** and **C**; Supplementary Fig. S4A). Consistently, there was a marked increase in the mRNA levels of *Hes1, Krt19, Epcam, Trop2*, and *Sox9* in the liver of $Alb^{cre}KP$; $Rosa^{NotchOE/+}$ mice compared with those of $Alb^{cre}KP$ mice (Supplementary Fig. S4B). Also, expression of pERK and the number of Ki67-positive cells were higher in the liver of $Alb^{cre}KP$; $Rosa^{NotchOE/+}$ mice compared with those of $Alb^{cre}KP$ mice (Supplementary Fig. S4C).

To evaluate the role of Hes1 in PDCs of $Alb^{cre}KP$; $Rosa^{NotchOE/+}$ mice, *Hes1* gene was knocked out by crossing $Hes1^{flox/flox}$ and $Alb^{cre}KP$; $Rosa^{NotchOE/+}$ mice. Histologic analysis showed a significant decrease in PDC marker–positive cells in $Alb^{cre}KP$; $Rosa^{NotchOE/+}$; $Hes1^{flox/flox}$ mice compared with that in $Alb^{cre}KP$; $Rosa^{NotchOE/+}$ mice at 8 weeks of age (**Fig. 3B** and **C**). mRNA levels of *Hes1*, as well as PDC markers levels, expression of pERK, and the number of Ki67-positive cells in the nontumorous liver tissues were also significantly decreased by *Hes1* deletion (Supplementary Fig. S4B and S4C). These findings indicate that Notch signaling strongly promoted PDC formation mainly via *Hes1*.

Consistently with PDC development, 66.7% (6/9) $Alb^{cre}KP$; $Rosa^{NotchOE/+}$ mice developed ICCs much earlier (at 8 weeks old) than $Alb^{cre}KP$ mice, indicating that Notch/Hes1 overexpression accelerated ICC development (**Fig. 3D**). As observed in PDCs, ICC in $Alb^{cre}KP$; $Rosa^{NotchOE/+}$ mice presented high Hes1 expression and were

Published OnlineFirst October 16, 2020; DOI: 10.1158/0008-5472.CAN-20-1161

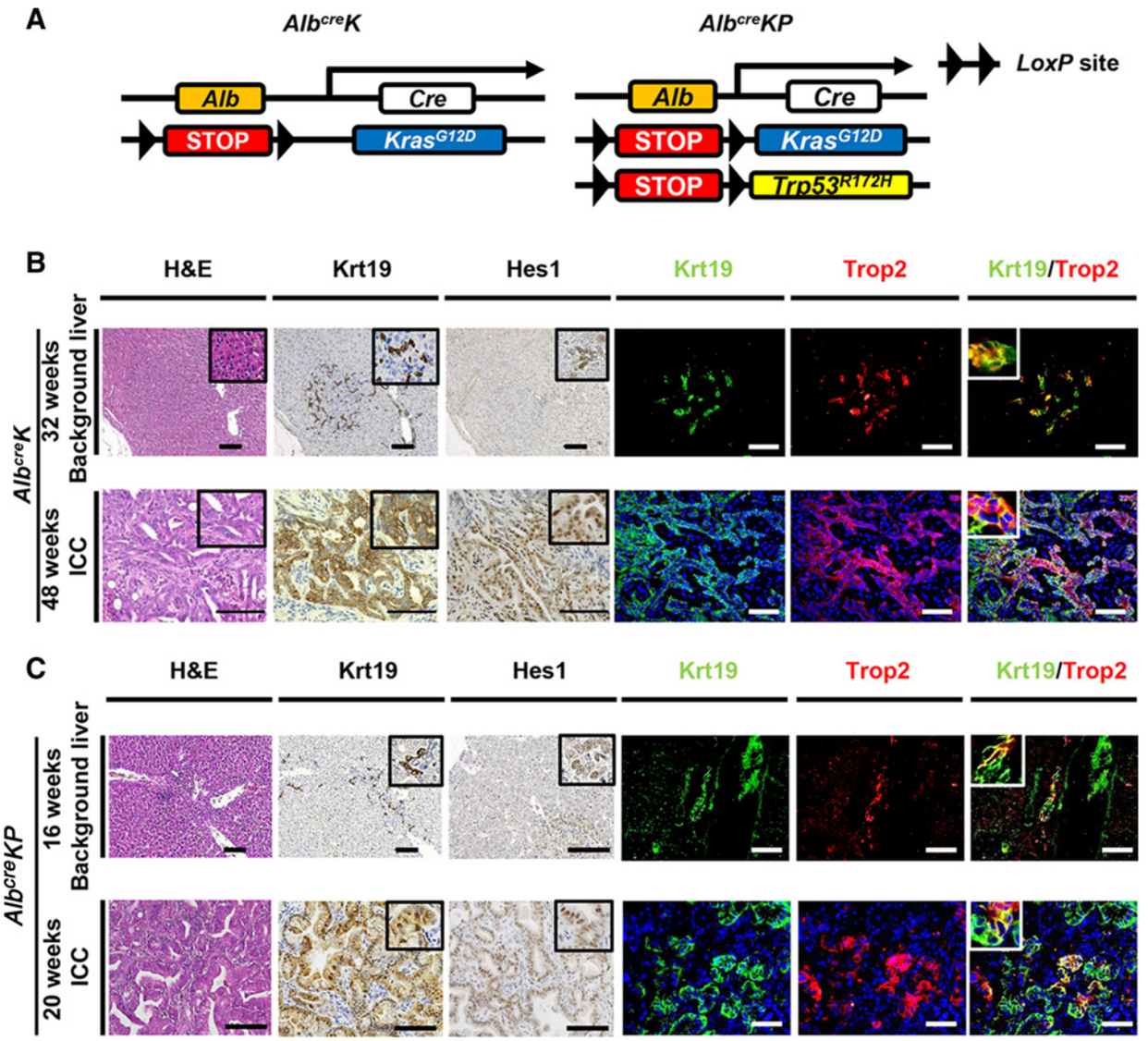

Figure 1.

Hes1-positive PDC formation was induced prior to development of *Kras*-driven ICC. **A,** The scheme of Cre-mediated liver-specific $Kras^{G12D}$ and $Trp53^{R172H}$ induction. **B,** Histologic analysis of liver sections in $Alb^{cre}K$ mice at 32 and 48 weeks of age. Representative images showing the results of hematoxylin and eosin (H&E) staining, IHC for Krt19 and Hes1, and immunofluorescent staining for Krt19 (green), Trop2 (red), and Hoechst (blue). Top plots, PDCs formed in background liver before ICC formation at 32 weeks of age. Bottom plots, ICC formed in the liver at 48 weeks of age. **C,** Histologic analysis of $Alb^{cre}KP$ mouse livers at 16 and 20 weeks of age. Representative images showing the results of hematoxylin and eosin staining, IHC for Krt19 and Hes1, and immunofluorescent staining for Krt19 (green), Trop2 (red), and Hoechst (blue). Top plots, PDCs formed in background liver before ICC formation at 16 weeks of age. Bottom plots, ICC formed in the liver at 16 weeks of age. Scale bars, 50 μm. *K*, $Kras^{G12D}$.

positive for Krt19, Epcam, Trop2, and Sox9 (Supplementary Fig. S5A). In contrast, ICC developed in only 9.1% (1/11) of 8-week-old $Alb^{cre}KP$; $Rosa^{NotchOE/+}$; $Hes1^{flox/flox}$ mice, indicating the abrogation of Notch1-mediated tumor induction following *Hes1* deletion (**Fig. 3D**). Expression of Hes1 was not observed in ICC formed with $Alb^{cre}KP$; $Rosa^{NotchOE/+}$; $Hes1^{flox/flox}$ mice (Supplementary Fig. S5B). In terms of HCC formation, the frequency of HCC development was similar between $Alb^{cre}KP$; $Rosa^{NotchOE/+}$; $Hes1^{WT/WT}$ and $Alb^{cre}KP$; $Rosa^{NotchOE/+}$; $Hes1^{flox/flox}$ mice (100%, 9/9 vs. 90.9%, 10/11, $P = 1$; Supplementary Fig. S5C). Together, these results suggest that activation of Notch signaling strongly promotes *Kras*-driven PDC proliferation as well as ICC development mainly via Hes1 activation.

Hes1 plays a role in DDC diet–induced PDC formation

To further examine the role of Hes1 in PDC development, we analyzed another mouse model in which PDCs were formed by DDC-mediated liver damage (25). First, we fed 0.1% DDC-containing chow to 4-week-old Alb^{cre}; $Hes1^{flox/flox}$ mice or control Alb^{cre}; $Hes1^{WT/WT}$ mice for 4 weeks (Supplementary Fig. S6A). We observed a substantial expansion of PDCs in Alb^{cre}; $Hes1^{WT/WT}$ mice but not in Alb^{cre}; $Hes1^{flox/flox}$ mice (Supplementary Fig. S6B). Quantification of the

Published OnlineFirst October 16, 2020; DOI: 10.1158/0008-5472.CAN-20-1161

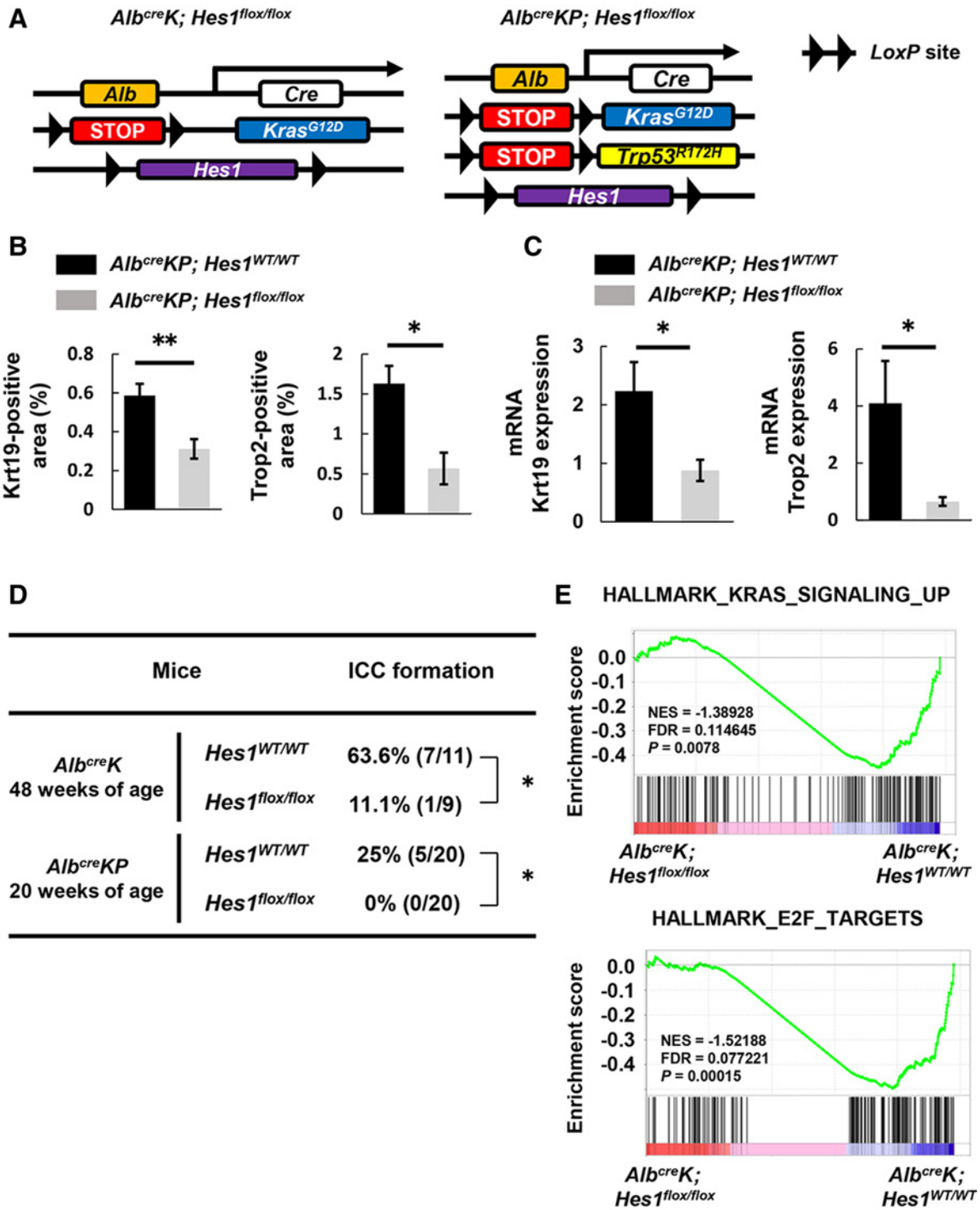

Figure 2.

Hes1 plays an important role in inducing PDC formation and ICC development. **A,** The scheme of Cre-mediated liver-specific *Kras*^{G12D} and *Trp53*^{R172H} induction and *Hes1* ablation. **B,** Percentages of Krt19- and Trop2-positive area per liver section in *Alb*^{cre}*KP* and *Alb*^{cre}*KP; Hes1*$^{flox/flox}$ mice. More than 5 mice were analyzed per group, and 15 fields were evaluated per mouse. **C,** Krt19 and Trop2 mRNA expression in nontumorous liver tissues of *Alb*^{cre}*KP* and *Alb*^{cre}*KP; Hes1*$^{flox/flox}$ mice. More than 5 mice were analyzed per group. **D,** Incidence of ICC in *Alb*^{cre}*K; Hes1*$^{WT/WT}$, *AlbcreK; Hes1*$^{flox/flox}$, *AlbcreKP; Hes1*$^{WT/WT}$, and *Alb*^{cre}*KP; Hes1*$^{flox/flox}$ mice. **E,** GSEA of genome-wide expression data using HALLMARK gene set of KRAS_SIGNALING_UP and HALLMARK_E2F_TARGETS of background liver tissue of *Alb*^{cre}*K; Hes1*$^{flox/flox}$ mice compared with *Alb*^{cre}*K; Hes1*$^{WT/WT}$ mice. Numbers in parentheses are the number of mice with tumors among the total mice examined. *, $P < 0.05$; **, $P < 0.01$, Student *t* test and χ^2 test. *K, Kras*^{G12D}. *KP, Kras*^{G12D}*; Trp53*^{R172H}. NES, normalized enrichment score.

Published OnlineFirst October 16, 2020; DOI: 10.1158/0008-5472.CAN-20-1161

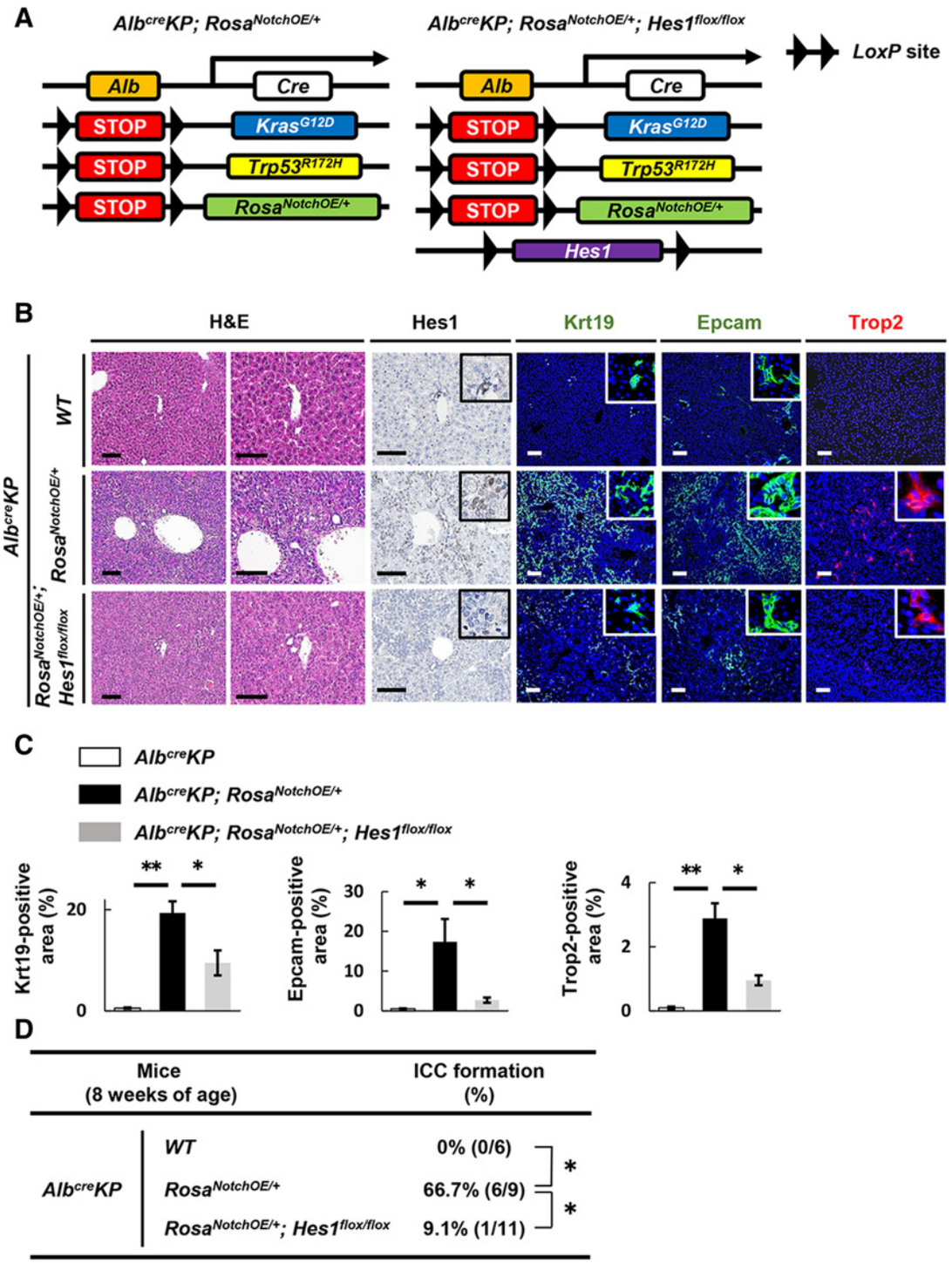

Figure 3.

Hes1 plays a central role in Notch1-induced PDC proliferation and ICC development. *Alb*^{cre}*KP, Alb*^{cre}*; Rosa*$^{NotchOE/+}$, and *Alb*^{cre}*KP; Rosa*$^{NotchOE/+}$*; Hes1*$^{flox/flox}$ mice were analyzed at 8 weeks of age. **A,** The scheme of Cre-mediated liver-specific induction of *Kras*^{G12D}, *Trp53*^{R172H}, and *Rosa*$^{NotchOE/+}$ induction and *Hes1* depletion. **B,** Images of hematoxylin and eosin (H&E) staining, IHC for Hes1 and immunofluorescence staining of Krt19 (green), Epcam (green), Trop2 (red), and Hoechst (blue) in PDCs in each mouse model. **C,** Percentages of Krt19-, Epcam-, and Trop2-positive areas per liver section in each mouse model. More than four mice were analyzed per group, and 15 fields were analyzed per mouse. **D,** Incidence of ICC in each mouse models. *, $P < 0.05$; **, $P < 0.01$, Student *t* test and χ^2 test. Scale bars, 50 μm. *KP, Kras*^{G12D}*; Trp53*^{R172H}.

Published OnlineFirst October 16, 2020; DOI: 10.1158/0008-5472.CAN-20-1161

Krt19- or Trop2-positive area confirmed a significant reduction of PDC formation in *Alb*^{cre}*; Hes1*$^{flox/flox}$ mice compared with that in *Alb*^{cre}*; Hes1*$^{WT/WT}$ mice (Supplementary Fig. S6C). These results suggest that Hes1 plays an essential role in PDC expansion in chronically damaged livers as well.

To further directly evaluate the role of Hes1 in promoting PDC formation, we crossed *Epcam-CreER*^{T2} *Tg* (*Epcam*^{creERT2}), *Rosa26-CAG-LSL-tdTomato-WPRE* (*Rosa*^{tdTomato}), and *Hes1*$^{flox/flox}$ mice. In these mice, *Hes1* deletion and genetic labeling by tdTomato in Epcam-positive PDCs could be induced via tamoxifen dependence (**Fig. 4A**). To obtain Cre recombination in Epcam-positive PDCs, PDCs were initially induced by 0.1% DDC diet feeding for a week, and tamoxifen was subsequently administered as previously reported (**Fig. 4B**). Genetic labeling of PDCs was confirmed by detection of tdTomato expression in PDCs positive for Krt19, Epcam, and Trop2 markers in *Epcam*^{creERT2}*; Rosa*^{tdTomato}*; Hes1*$^{WT/WT}$ mice at 6 weeks after initiating the DDC diet (**Fig. 4B**–**D**). In contrast, tdTomato-positive PDCs were significantly reduced in *Epcam*^{creERT2}*; Rosa*^{tdTomato}*; Hes1*$^{flox/flox}$ mice fed with DDC diet ($P = 0.007$; **Fig. 4D** and **E**), indicating that *Hes1* deletion suppressed PDC expansion. Supporting this data, most of the PDCs observed in *Epcam*^{creERT2}*; Rosa*^{tdTomato}*; Hes1*$^{flox/flox}$ mice fed the DDC diet were positive for Hes1 expression because of insufficient Cre recombination efficiency (**Fig. 4D**). These findings confirm that Hes1 plays a crucial role also in inducing PDC formation in the chronically damaged liver.

DDC diet–induced and *Kras*-driven ICC originates from Hes1-positive PDCs

PDC expansions prior to ICC development and the similar expression patterns between PDCs and ICCs in the *Kras*-driven mouse models suggest that ICCs could have originated from PDCs. The similar effects of the Notch/Hes1 axis on PDC formation and ICC development supported this prediction. To determine whether Hes1-positive PDCs transformed into ICC, we generated *Epcam*^{creERT2}*KP; Rosa*$^{NotchOE/tdTomato}$ mice in which expression of *Kras*^{G12D}, *Trp53*^{R172H}, *NotchOE*, and *tdTomato* was specifically induced in Epcam-positive PDCs in a tamoxifen-dependent manner (**Fig. 5A**). Administration of DDC diet followed by tamoxifen-induced genetic recombination PDCs, which was confirmed at 16 and 24 weeks of age (**Fig. 5B** and **C**). Importantly, the development of tdTomato-positive ICCs, as well as premalignant lesions, was observed at 24 weeks of age (**Fig. 5C**). These results confirm that DDC diet-induced Hes1-positive PDCs give rise to premalignant lesions and subsequent ICCs.

HES1 expression is correlated with the development of human ICCs

Finally, we analyzed the involvement of HES1 in the development and progression of human ICCs. The characteristics of analyzed patients with ICC are shown in Supplementary Table S4. Histologic and IHC analyses revealed that nontumorous liver tissues of patients with ICC harbor a significantly higher number of PDCs positive for Keratin 19 and HES1 markers than those with metastatic liver tumors ($P = 0.022$; **Fig. 6A**), suggesting a close association between PDC formation and ICC development in humans. Significant HES1 expression was also noted in 52.0% (13/25) of human ICC cases, but only in 9.5% (2/21) of HCC cases ($P = 0.004$; **Fig. 6B** and **C**). Taken together, these results suggest that HES1 is also closely involved in the proliferation of human PDCs and the subsequent development of ICC in humans.

Discussion

Despite reports that human ICC profoundly expresses molecules involved in the Notch signaling pathway, including *Hes1* (16, 39), the detailed mechanisms by which Notch signaling mediates the development of ICC remain unclear. In the present study, utilizing genetically engineered mouse models and human samples, we demonstrated that Hes1 plays an essential role in promoting PDC formation and the subsequent development of ICC. We also showed that DDC diet–induced Hes1-expressing PDCs give rise to ICCs.

PDCs are often observed as ductular reactions in the liver with chronic inflammation and are considered to function as liver stem/progenitor cells (25). Studies of genetically engineered mouse models showed that Notch signaling is involved in ductular reactions (16). In the present study, we found higher numbers of PDCs in livers with increased Hes1 expression in the presence of chronic liver injury or oncogenic *Kras* mutation. This is the first report showing that oncogenic mutations, including *Kras*, cause ductular cell expansion. Although the mechanisms underlying the oncogenic transformation of proliferating PDCs remain unknown, the two recent articles reported that mutated *Kras* activation caused a premalignant proliferation of ductal cells via *Hes1* activation in the pancreas, which is consistent with our findings (40, 41). We demonstrated here that *Kras*-driven PDC proliferation was strongly promoted by Notch1 overexpression, but significantly suppressed by *Hes1* deletion. The reduced PDC proliferation by specific *Hes1* deletion in *Epcam*^{creERT2} mice further confirmed the essential role of Hes1 in these cells. These findings suggest that Hes1 plays a crucial role in the expansions of PDCs induced by oncogenic *Kras* mutation or chronic inflammation. On the other hand, our RNA-seq analysis and IHC using nonneoplastic background liver tissues of *Alb*^{cre}*K; Hes1*$^{WT/WT}$ and *Alb*^{cre}*K; Hes1*$^{flox/flox}$ mice revealed attenuated RAS/ERK signaling in *Alb*^{cre}*K; Hes1*$^{WT/WT}$ mice despite the same status of *Kras* mutation between the two strains. These findings suggest a role of Hes1 in maintaining activation of the RAS/ERK pathway. Considering that Hes1 is a transcriptional repressor, it is possible that repression of genes that block the RAS/ERK pathway contributes to the activation of the pathway. Indeed, among the 170 DEGs, *FOXO3A* gene, which was identified as a suppressor of the RAS/ERK pathway (42), was elevated by Hes1 depletion. Given the discussion described above, mutant *Kras* may induce Hes1 expression, which in turn could be required for maintaining activation of the RAS/ERK pathway, and these synergistic effects of mutant *Kras* and Hes1 may induce PDCs. *Hes1* deletion also suppressed E2F pathway, which controls the cell-cycle progression in various cancers including ICC (43).

Oncogenic mutations in *Kras* and *Trp53* genes have been reported to promote ICC development in both humans and mice (9, 10). Utilizing *Kras/Trp53*-mediated ICC mouse models, we showed here that *Hes1* is upregulated in ICC. Similar to the induction of PDC proliferation, ICC development was strongly promoted by Notch1 overexpression but inhibited by Hes1 deletion, suggesting an involvement of the Notch/Hes1 axis in ICC development. Jeliazkova and colleagues demonstrated that overexpression of Notch2 also induces ductular reaction with Hes1 activation (44). However, unlike Notch1, this phenotype was not inhibited by Hes1 deletion. There can be several reasons for this difference between Notch1 and Notch2. One reason is that dependence on Hes1 in this phenotype may differ between the two receptors. The phenotype of Notch2 overexpression was canceled by genetic inactivation of *Rbpj*, suggesting that molecules downstream of canonical Notch2 signaling other than Hes1 could compensate the loss of Hes1 (44). In contrast, Notch1 overexpression

Published OnlineFirst October 16, 2020; DOI: 10.1158/0008-5472.CAN-20-1161

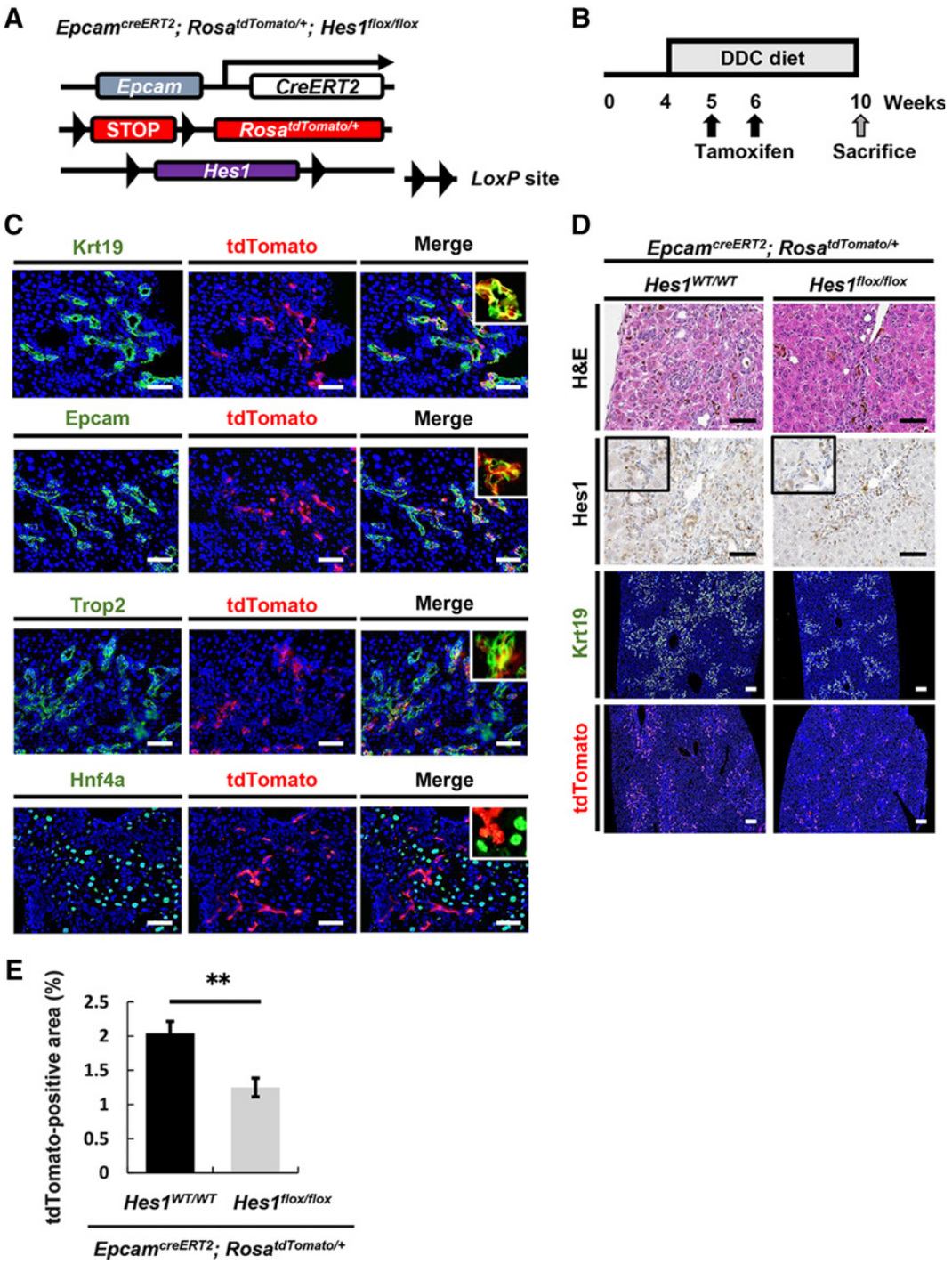

Figure 4.

Hes1 plays a role in DDC diet–induced PDC formation. **A,** The scheme of tamoxifen-induced Cre-mediated PDCs-specific *Rosa*^{tdTomato} induction and *Hes1* depletion. **B,** Schematic diagram of the experimental design. **C,** Analysis of tdTomato expression (red) together with immunofluorescence staining for Krt19 (green), Epcam (green), Trop2 (green), Hnf4a(green), and Hoechst (blue) in the liver sections of *Epcam*^{creERT2}; *Rosa*^{tdTomato} mice fed a DDC diet for 6 weeks. **D,** Histologic analysis of liver sections in *Epcam*^{creERT2}; *Rosa*^{tdTomato}; *Hes1*$^{WT/WT}$ and *Epcam*^{creERT}; *Rosa*^{tdTomato}; *Hes1*$^{flox/flox}$ mice. Representative images showing the results of hematoxylin and eosin staining (H&E), IHC for Hes1 and immunofluorescence staining for Krt19 (green), Hoechst (blue), and tdTomato expression (red). **E,** tdTomato-positive area per liver section in *Epcam*^{creERT}; *Rosa*^{tdTomato}; *Hes1*$^{WT/WT}$ and *Epcam*^{creERT2}; *Rosa*^{tdTomato}; *Hes1*$^{flox/flox}$ mice. More than 5 mice were analyzed per group, and 15 fields were counted per mouse. **, $P < 0.01$, Student t test. Scale bars, 50 μm.

Published OnlineFirst October 16, 2020; DOI: 10.1158/0008-5472.CAN-20-1161

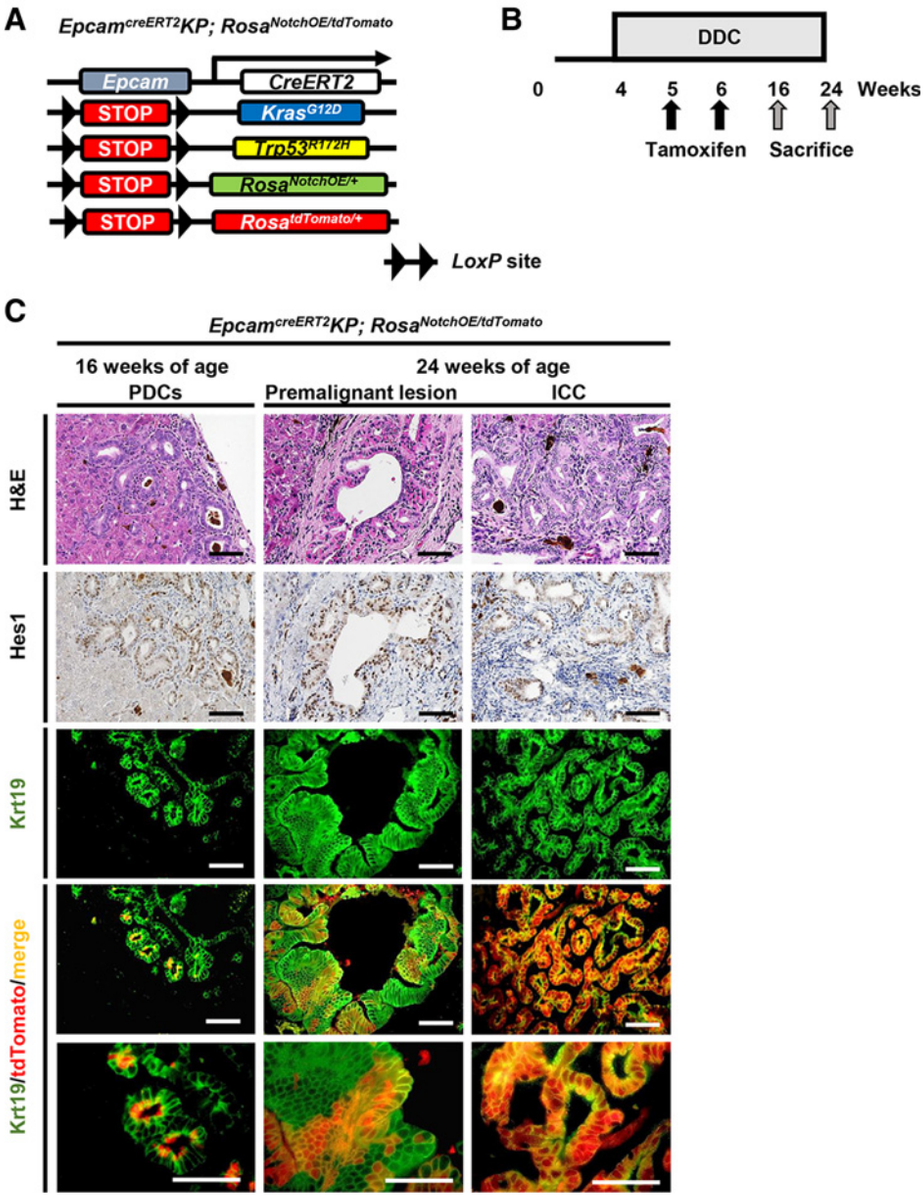

Figure 5.

Kras-driven ICC originates from Hes1-positive PDCs. **A,** The scheme of tamoxifen-induced Cre-mediated PDC-specific induction of $Kras^{G12D}$, $Trp53^{R172H}$, $Rosa^{NotchOE}$, and $Rosa^{tdTomato}$ mice. **B,** Schematic diagram of the experimental design. **C,** Histologic analysis of the liver sections from $Epcam^{creERT2}KP;\ Rosa^{NotchOE/tdTomato}$ mice. Images of hematoxylin and eosin (H&E) staining, IHC of Hes1, and immunofluorescence staining of Krt19 (green) and tdTomato (red) in PDCs, premalignant lesion, and ICC. Scale bars, 50 μm. *KP*, $Kras^{G12D}$;$Trp53^{R172H}$.

may have higher Hes1 dependency. Another reason is the difference in experimental models. We have previously shown that MAPK activated by mutant *Kras* induces Hes1 in a Notch signaling–independent manner (41), suggesting that our *Kras*-driven mouse cancer model may exhibit more Hes1 dependency. Consistently, some studies have shown that the Notch/Hes1 axis is involved in the development of biliary tract cancers, including extrahepatic bile duct and gallbladder cancers (45, 46). In contrast, HCC development was not affected by *Hes1* deletion in our study. Given that upregulation of Notch signaling molecules has been reported in HCCs and ICCs, downstream molecules of Notch signaling other than Hes1 may play a role in HCC development (17, 18). Collectively, our findings indicate that *Hes1* plays a central role as a Notch effector in ICC development.

Our findings that PDC proliferation was induced prior to ICC development and that both ICCs and PDCs expressed ductal markers regulated by Hes1 suggest that PDCs can transform into ICCs. This conclusion was confirmed by lineage tracing experiments using $Epcam^{creERT2}$ mice showing that DDC diet–induced PDCs transformed into premalignant lesions and subsequently into ICCs. In agreement with our previous study showing that HCCs originate from PDCs (28), our data showed that PDCs could also lead to both cholangiocellular and hepatocellular cancers. Consistently, Holczabauer and colleagues reported that stable expression of oncogenic H-Ras and SV40LT in liver progenitor cells led to both ICC and HCC development and that Epcam-positive liver progenitor cells had high tumorigenic potential (47). Thus, in this study, we provide novel evidence that ICCs could originate from PDCs via regulation of *Hes1* expression.

Finally, we analyzed human ICC specimens. Previous reports showed that SOX9 is a key progenitor marker of the intrahepatic

Published OnlineFirst October 16, 2020; DOI: 10.1158/0008-5472.CAN-20-1161

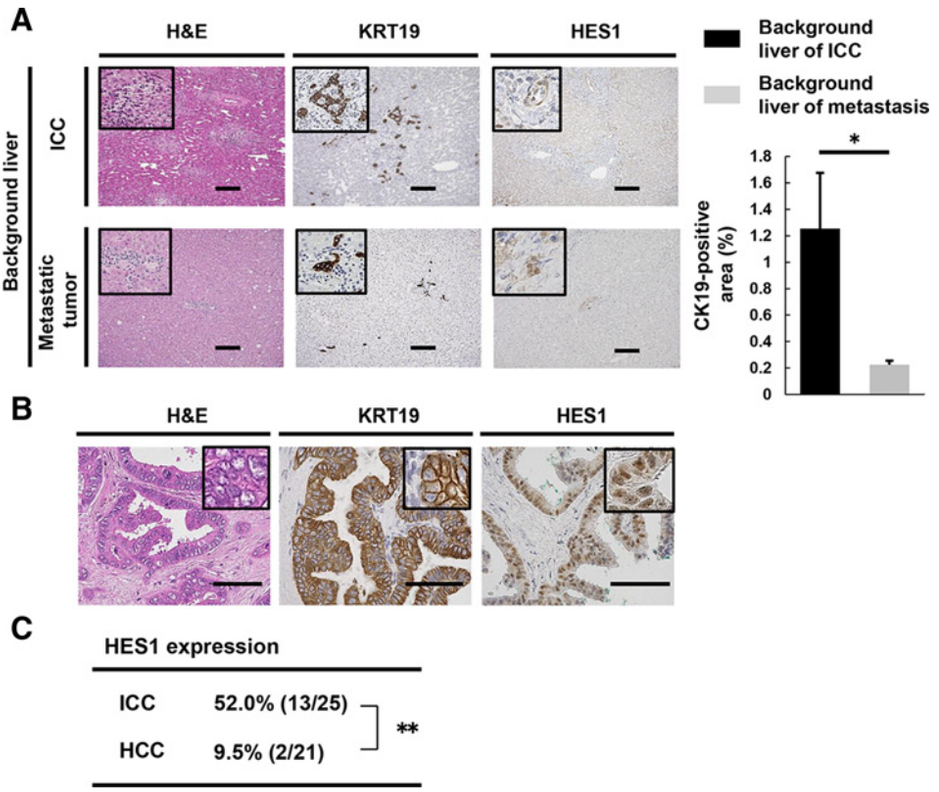

Figure 6.

HES1 is involved in the development of human ICCs. **A,** Histologic analysis of nontumorous liver tissues in patients with ICC and metastatic liver cancers. Representative images showing the results of hematoxylin and eosin (H&E) staining, and IHC for KRT19 and HES1. Percentages of KRT19-positive areas per liver section were evaluated. **B,** Hematoxylin and eosin staining and IHC for KRT19 and HES1 in human ICC tissues. **C,** HES1 expression in human ICC and HCC cases. Numbers in parentheses are the number of HES1-positive ICC and HCC cases among the total cases examined. *, $P < 0.05$; **, $P < 0.01$, Student t test and χ^2 test. Scale bars, 50 μm.

bile duct and is deeply involved in the initiation of ICC (10, 48); this is consistent with our finding that ICC is derived from PDCs. Interestingly, higher numbers of HES1-positive PDCs were observed in the nontumorous liver tissue of patients with ICCs and rarely found in metastatic liver cancers in humans. These findings suggest that HES1 is also closely involved in PDC formation and the subsequent development of ICC in humans. However, it is possible that increased PDCs are a result of local liver inflammation induced by ICCs, and further investigation is needed to clarify the relationship between PDC formation and ICC development.

Numerous clinical studies targeting Notch signaling in various tumors using inhibitors are currently underway (49). Our results and those of others suggest that the Notch signaling pathway may be a useful therapeutic target in ICCs (39). However, broad inhibition of the Notch signaling pathway causes some severe adverse events, such as skin cancers (50). In contrast, we previously reported that specific inhibition of Hes1 in mice elicited a tumor-suppressing effect on pancreatic cancer cells without severe adverse events (20). In this study, liver-specific *Hes1* deletion did not affect the healthy liver development. Therefore, targeting a key effector, such as Hes1, rather than the complete blockade of Notch signaling, can provide effective tumor suppression with reduced adverse events in ICC. There are two limitations of our study. First, we could not discriminate PDC formation and cell viability. Second, we could not confirm in our mouse models whether PDCs originate from hepatocytes, bile duct epithelium, or stem cells of the liver.

In conclusion, we elucidated a novel role for Hes1 in promoting PDC formation and ICC development. Furthermore, we demonstrated that PDCs can transform into ICC and that Hes1 plays an essential role in such PDC-mediated ICC development. These findings provide valuable insights for the development of new effective methods for preventing or treating ICC.

Authors' Disclosures

R. Kageyama reports grants from a government agency during the conduct of the study and grants from a foundation outside the submitted work. No disclosures were reported by the other authors.

Authors' Contributions

T. Matsumori: Conceptualization, formal analysis, validation, investigation, visualization, writing-original draft, writing-review and editing. **Y. Kodama:** Supervision, writing-review and editing. **A. Takai:** Supervision, investigation. **M. Shiokawa:** Supervision, investigation. **Y. Nishikawa:** Investigation. **T. Matsumoto:** Investigation. **H. Takeda:** Formal Analysis, Investigation. **S. Marui:** Investigation. **H. Okada:** Investigation. **T. Hirano:** Investigation. **T. Kuwada:** Investigation. **Y. Sogabe:** Investigation. **N. Kakiuchi:** Investigation. **T. Tomono:** Investigation. **A. Mima:** Investigation. **T. Morita:** Investigation. **T. Ueda:** Investigation. **M. Tsuda:** Investigation. **Y. Yamauchi:** Investigation. **K. Kuriyama:** Investigation. **Y. Sakuma:** Investigation. **Y. Ota:** Investigation. **T. Maruno:** Investigation. **N. Uza:** Investigation. **H. Marusawa:** Investigation. **R. Kageyama:** Investigation. **T. Chiba:** Investigation. **H. Seno:** Supervision, Investigation.

Acknowledgments

We wish to thank Yuta Kawamata and Taichi Ito for their excellent technical support during our research. This work was supported by the JSPS and MEXT KAKENHI grant numbers 15J05143, 16K09395, and 17H06803.

The costs of publication of this article were defrayed in part by the payment of page charges. This article must therefore be hereby marked *advertisement* in accordance with 18 U.S.C. Section 1734 solely to indicate this fact.

Received April 10, 2020; revised August 11, 2020; accepted October 13, 2020; published first October 16, 2020.

References

1. Jemal A, Bray F, Center MM, Ferlay J, Ward E, Forman D. Global cancer statistics. CA Cancer J Clin 2011;61:69–90.
2. Thinkhamrop K, Khuntikeo N, Phonjitt P, Chamadol N, Thinkhamrop B, Moore MA, et al. Association between diabetes mellitus and fatty liver based on ultrasonography screening in the world's highest cholangiocarcinoma incidence region, Northeast Thailand. Asian Pac J Cancer Prev 2015;16: 3931–6.
3. Navas MC, Glaser S, Dhruv H, Celinski S, Alpini G, Meng F. Hepatitis C virus infection and cholangiocarcinoma: an insight into epidemiologic evidences and hypothetical mechanisms of oncogenesis. Am J Pathol 2019;189:1122–32.
4. Zhang H, Yang T, Wu M, Shen F. Intrahepatic cholangiocarcinoma: epidemiology, risk factors, diagnosis and surgical management. Cancer Lett 2016;379: 198–205.
5. Chiba T, Marusawa H, Ushijima T. Inflammation-associated cancer development in digestive organs: mechanisms and roles for genetic and epigenetic modulation. Gastroenterology 2012;143:550–63.
6. Nakamura H, Arai Y, Totoki Y, Shirota T, Elzawahry A, Kato M, et al. Genomic spectra of biliary tract cancer. Nat Genet 2015;47:1003–10.
7. Schulze K, Imbeaud S, Letouze E, Alexandrov LB, Calderaro J, Rebouissou S, et al. Exome sequencing of hepatocellular carcinomas identifies new mutational signatures and potential therapeutic targets. Nat Genet 2015;47:505–11.
8. Guest RV, Boulter L, Kendall TJ, Minnis-Lyons SE, Walker R, Wigmore SJ, et al. Cell lineage tracing reveals a biliary origin of intrahepatic cholangiocarcinoma. Cancer Res 2014;74:1005–10.
9. O'Dell MR, Huang JL, Whitney-Miller CL, Deshpande V, Rothberg P, Grose V, et al. Kras(G12D) and p53 mutation cause primary intrahepatic cholangiocarcinoma. Cancer Res 2012;72:1557–67.
10. Hill MA, Alexander WB, Guo B, Kato Y, Patra KC, O'Dell MR, et al. Kras and Tp53 mutations cause cholangiocyte- and hepatocyte-derived cholangiocarcinoma. Cancer Res 2018;78:4445–51.
11. Geisler F, Strazzabosco M. Emerging roles of Notch signaling in liver disease. Hepatology 2015;61:382–92.
12. Kodama Y, Hijikata M, Kageyama R, Shimotohno K, Chiba T. The role of notch signaling in the development of intrahepatic bile ducts. Gastroenterology 2004; 127:1775–86.
13. Huntzicker EG, Hotzel K, Choy L, Che L, Ross J, Pau G, et al. Differential effects of targeting Notch receptors in a mouse model of liver cancer. Hepatology 2015; 61:942–52.
14. Zhang S, Wang J, Wang H, Fan L, Fan B, Zeng B, et al. Hippo cascade controls lineage commitment of liver tumors in mice and humans. Am J Pathol 2018;188: 995–1006.
15. Wang J, Dong M, Xu Z, Song X, Zhang S, Qiao Y, et al. Notch2 controls hepatocyte-derived cholangiocarcinoma formation in mice. Oncogene 2018;37: 3229–42.
16. Zender S, Nickeleit I, Wuestefeld T, Sorensen I, Dauch D, Bozko P, et al. A critical role for notch signaling in the formation of cholangiocellular carcinomas. Cancer Cell 2013;23:784–95.
17. Guest RV, Boulter L, Dwyer BJ, Kendall TJ, Man TY, Minnis-Lyons SE, et al. Notch3 drives development and progression of cholangiocarcinoma. Proc Natl Acad Sci U S A 2016;113:12250–5.
18. Villanueva A, Alsinet C, Yanger K, Hoshida Y, Zong Y, Toffanin S, et al. Notch signaling is activated in human hepatocellular carcinoma and induces tumor formation in mice. Gastroenterology 2012;143:1660–9.
19. Gao J, Xiong Y, Wang Y, Wang Y, Zheng G, Xu H. Hepatitis B virus X protein activates Notch signaling by its effects on Notch1 and Notch4 in human hepatocellular carcinoma. Int J Oncol 2016;48:329–37.
20. Perron A, Nishikawa Y, Iwata J, Shimojo H, Takaya J, Kobayashi K, et al. Small-molecule screening yields a compound that inhibits the cancer-associated transcription factor Hes1 via the PHB2 chaperone. J Biol Chem 2018;293: 8285–94.
21. Arai MA, Ishikawa N, Tanaka M, Uemura K, Sugimitsu N, Suganami A, et al. Hes1 inhibitor isolated by target protein oriented natural products isolation (TPO-NAPI) of differentiation activators of neural stem cells. Chem Sci 2016;7: 1514–20.
22. Sia D, Villanueva A, Friedman SL, Llovet JM. Liver cancer cell of origin, molecular class, and effects on patient prognosis. Gastroenterology 2017;152: 745–61.
23. Fan B, Malato Y, Calvisi DF, Naqvi S, Razumilava N, Ribback S, et al. Cholangiocarcinomas can originate from hepatocytes in mice. J Clin Invest 2012;122:2911–5.
24. Jors S, Jeliazkova P, Ringelhan M, Thalhammer J, Durl S, Ferrer J, et al. Lineage fate of ductular reactions in liver injury and carcinogenesis. J Clin Invest 2015; 125:2445–57.
25. Miyajima A, Tanaka M, Itoh T. Stem/progenitor cells in liver development, homeostasis, regeneration, and reprogramming. Cell Stem Cell 2014;14: 561–74.
26. Shin S, Upadhyay N, Greenbaum LE, Kaestner KH. Ablation of Foxl1-Cre-labeled hepatic progenitor cells and their descendants impairs recovery of mice from liver injury. Gastroenterology 2015;148:192–202.
27. Miura Y, Matsui S, Miyata N, Harada K, Kikkawa Y, Ohmuraya M, et al. Differential expression of Lutheran/BCAM regulates biliary tissue remodeling in ductular reaction during liver regeneration. eLife 2018;7:e36572.
28. Matsumoto T, Takai A, Eso Y, Kinoshita K, Manabe T, Seno H, et al. Proliferating EpCAM-positive ductal cells in the inflamed liver give rise to hepatocellular carcinoma. Cancer Res 2017;77:6131–43.
29. Boulter L, Govaere O, Bird TG, Radulescu S, Ramachandran P, Pellicoro A, et al. Macrophage-derived Wnt opposes Notch signaling to specify hepatic progenitor cell fate in chronic liver disease. Nat Med 2012;18:572–9.
30. Eso Y, Takai A, Matsumoto T, Inuzuka T, Horie T, Ono K, et al. MSH2 dysregulation is triggered by proinflammatory cytokine stimulation and is associated with liver cancer development. Cancer Res 2016;76: 4383–93.
31. Imayoshi I, Shimogori T, Ohtsuka T, Kageyama R. Hes genes and neurogenin regulate non-neural versus neural fate specification in the dorsal telencephalic midline. Development 2008;135:2531–41.
32. Jackson EL, Willis N, Mercer K, Bronson RT, Crowley D, Montoya R, et al. Analysis of lung tumor initiation and progression using conditional expression of oncogenic K-ras. Genes Dev 2001;15:3243–8.
33. Olive KP, Tuveson DA, Ruhe ZC, Yin B, Willis NA, Bronson RT, et al. Mutant p53 gain of function in two mouse models of Li-Fraumeni syndrome. Cell 2004; 119:847–60.
34. Madisen L, Zwingman TA, Sunkin SM, Oh SW, Zariwala HA, Gu H, et al. A robust and high-throughput Cre reporting and characterization system for the whole mouse brain. Nat Neurosci 2009;13:133–40.
35. Murtaugh LC, Stanger BZ, Kwan KM, Melton DA. Notch signaling controls multiple steps of pancreatic differentiation. Proc Natl Acad Sci U S A 2003;100: 14920–5.
36. Ito T, Udaka N, Yazawa T, Okudela K, Hayashi H, Sudo T, et al. Basic helix-loop-helix transcription factors regulate the neuroendocrine differentiation of fetal mouse pulmonary epithelium. Development 2000; 127:3913–21.
37. Okabe M, Tsukahara Y, Tanaka M, Suzuki K, Saito S, Kamiya Y, et al. Potential hepatic stem cells reside in EpCAM+ cells of normal and injured mouse liver. Development 2009;136:1951–60.
38. Yamashita T, Wang XW. Cancer stem cells in the development of liver cancer. J Clin Invest 2013;123:1911–8.
39. O'Rourke CJ, Matter MS, Nepal C, Caetano-Oliveira R, Ton PT, Factor VM, et al. Identification of a pan-gamma-secretase inhibitor response signature for Notch-driven cholangiocarcinoma. Hepatology 2020;71: 196–213.
40. Hidalgo-Sastre A, Brodylo RL, Lubeseder-Martellato C, Sipos B, Steiger K, Lee M, et al. Hes1 controls exocrine cell plasticity and restricts development of pancreatic ductal adenocarcinoma in a mouse model. Am J Pathol 2016;186: 2934–44.
41. Nishikawa Y, Kodama Y, Shiokawa M, Matsumori T, Marui S, Kuriyama K, et al. Hes1 plays an essential role in Kras-driven pancreatic tumorigenesis. Oncogene 2019;38:4283–96.
42. Cheong JK, Zhang F, Chua PJ, Bay BH, Thorburn A, Virshup DM. Casein kinase 1alpha-dependent feedback loop controls autophagy in RAS-driven cancers. J Clin Invest 2015;125:1401–18.
43. Kent LN, Leone G. The broken cycle: E2F dysfunction in cancer. Nat Rev Cancer 2019;19:326–38.
44. Jeliazkova P, Jors S, Lee M, Zimber-Strobl U, Ferrer J, Schmid RM, et al. Canonical Notch2 signaling determines biliary cell fates of embryonic hepatoblasts and adult hepatocytes independent of Hes1. Hepatology 2013;57:2469–79.
45. Aoki S, Mizuma M, Takahashi Y, Haji Y, Okada R, Abe T, et al. Aberrant activation of Notch signaling in extrahepatic cholangiocarcinoma:

Published OnlineFirst October 16, 2020; DOI: 10.1158/0008-5472.CAN-20-1161

clinicopathological features and therapeutic potential for cancer stem cell-like properties. BMC Cancer 2016;16:854.
46. Chung WC, Wang J, Zhou Y, Xu K. Kras(G12D) upregulates Notch signaling to induce gallbladder tumorigenesis in mice. Oncoscience 2017;4:131–8.
47. Holczbauer A, Factor VM, Andersen JB, Marquardt JU, Kleiner DE, Raggi C, et al. Modeling pathogenesis of primary liver cancer in lineage-specific mouse cell types. Gastroenterology 2013;145:221–31.
48. Kawaguchi Y. Sox9 and programming of liver and pancreatic progenitors. J Clin Invest 2013;123:1881–6.
49. Andersson ER, Lendahl U. Therapeutic modulation of Notch signalling–are we there yet? Nat Rev Drug Discov 2014;13:357–78.
50. Doody RS, Raman R, Sperling RA, Seimers E, Sethuraman G, Mohs R, et al. Peripheral and central effects of gamma-secretase inhibition by semagacestat in Alzheimer's disease. Alzheimers Res Ther 2015;7:36.

Cancer Research
The Journal of Cancer Research (1916–1930) | The American Journal of Cancer (1931–1940)

AACR American Association for Cancer Research

Hes1 Is Essential in Proliferating Ductal Cell –Mediated Development of Intrahepatic Cholangiocarcinoma

Tomoaki Matsumori, Yuzo Kodama, Atsushi Takai, et al.

Cancer Res 2020;80:5305-5316. Published OnlineFirst October 16, 2020.